Journal of Complex Networks (2014) **2**, 110–120
doi:10.1093/comnet/cnt019
Advance Access publication on 9 January 2014

Robustness of skeletons and salient features in networks

Louis M. Shekhtman[†]
Department of Physics, Bar-Ilan University, Ramat Gan 52900, Israel and Department of Physics and Astronomy, Northwestern University, Evanston, IL 60208, USA
[†]Corresponding author. Email: lsheks@gmail.com

James P. Bagrow
Department of Mathematics and Statistics, Vermont Advanced Computing Center, Complex Systems Center, University of Vermont, Burlington, VT 05405, USA and Department of Engineering Sciences and Applied Mathematics, Northwestern Institute on Complex Systems, Northwestern University, Evanston, IL 60208, USA

and

Dirk Brockmann
Robert-Koch-Institute, Seestrasse 10, 13353 Berlin, Germany, Department of Biology, Humboldt-University Berlin, Invalidenstrasse 42, 10115 Berlin, Germany and Department of Engineering Sciences and Applied Mathematics, Northwestern Institute on Complex Systems, Northwestern University, Evanston, IL 60208, USA

Edited by: Raissa D'Souza

[Received on 2 September 2013; accepted on 28 November 2013]

Real-world network datasets often contain a wealth of complex topological information. In the face of these data, researchers often employ methods to extract reduced networks containing the most important structures or pathways, sometimes known as 'skeletons' or 'backbones'. Numerous such methods have been developed. Yet data are often noisy or incomplete, with unknown numbers of missing or spurious links. Relatively little effort has gone into understanding how salient network extraction methods perform in the face of noisy or incomplete networks. We study this problem by comparing how the salient features extracted by two popular methods change when networks are perturbed, either by deleting nodes or links, or by randomly rewiring links. Our results indicate that simple, global statistics for skeletons can be accurately inferred even for noisy and incomplete network data, but it is crucial to have complete, reliable data to use the exact topologies of skeletons or backbones. These results also help us understand how skeletons respond to damage to the network itself, as in an attack scenario.

Keywords: mathematical and numerical analysis of networks; network stability under perturbation and duress; network percolation; centrality measures; network skeletons and backbones.

1. Introduction

Many systems consist of discrete elements that are coupled to one another in complex ways. Modelling these systems as networks often exposes more clearly the fundamental properties of the dataset [1–5]. While modelling systems as networks is not a new approach, it has become more prevalent due to the

TABLE 1 *Summary of the networks. Presented here*: N, *the number of nodes in the network*; L, *the number of links*; $\langle k \rangle$, *the average degree*; $\mathrm{CV}(k)$ *the coefficient of variation of degree*; $\mathrm{CV}(w)$, *the coefficient of variation of weight*; $\rho = L/\binom{N}{2}$, *the network density and* r, *the degree assortativity coefficient. The coefficients of variation* $\mathrm{CV}(w)$ *and* $\mathrm{CV}(k)$ *are defined as the ratio of the standard deviation,* σ, *to the mean,* μ, *of the weight and degree populations, respectively*

Network	N	L	$\langle k \rangle$	ρ	$\mathrm{CV}(k)$	$\mathrm{CV}(w)$	r
Airport	1227	18050	29.42	0.024	1.29	2.25	−0.06
Migration	3056	71551	46.83	0.015	1.94	6.13	−0.06
Cargo	951	25819	54.30	0.057	1.22	6.85	−0.14
Neural	297	2141	14.46	0.049	0.89	1.35	−0.16
Food Web	121	1763	29.14	0.24	0.45	11.77	−0.10
Metabolic	311	1304	8.39	0.027	1.79	7.91	−0.25
Random	1000	15028	30.06	0.03	0.177	1.44	−0.005

greater availability of large datasets [6]. The brain's neurons have been mapped using these methods [7], as have air traffic patterns [8], and the flow of cargo throughout the world [9].

The explosion of research on complex networks in recent years has led to the discovery of various properties of networks and has allowed us to find ways of reducing the complexity while preserving certain key features. Many of these methods focus on reducing the number of nodes in the network. Aside from simple thresholding, more sophisticated coarse-graining techniques have also been used [10] to reduce the number of distinct entities in the network. Here, we will focus on methods of reducing the number of links in the network while preserving the nodes. This is advantageous since it reduces the complexity of the system while still preserving scale-free properties.

Further, there has been considerable effort in understanding how networks as a whole respond to damage [11–14]. These studies have explored different methods of perturbing the network such as intentional attack and random failure.

Despite the significant amount of research in both of these areas separately, there has been little work in combining the study of backbone and skeleton methods with stress applied to the system. Here, we examine how skeletons and backbones respond to different methods of stress applied to the system.

1.1 *Network data*

In exploring the response of network skeletons to perturbations to the network as a whole, we use three different transportation networks, three biological networks and one network model. The transportation networks used are the world air transportation network from 1995 (Airport), the network of global cargo shipments (Cargo) and the network of human migrations provided by the Internal Revenue Service (Migration). The Airport network was taken from OAG Worldwide Ltd and has been examined in various previous studies [8,15,16]. The Cargo network comes from the IHS Fairplay data and contains information about 16323 container ships [9].

For biological networks, we examine the network containing the neural interactions of *Caenorhabditis elegans* (Neural), the Florida Bay food web (Food Web) and the metabolic network of *Escherichia coli* (Metabolic). The Neural network comes from work by White *et al.* [17] and was explored in Watts and Strogatz [18]. The Food Web is from a collection of public datasets available online [19]. Finally, the Metabolic network comes from experimental research and has also been previously analysed [20].

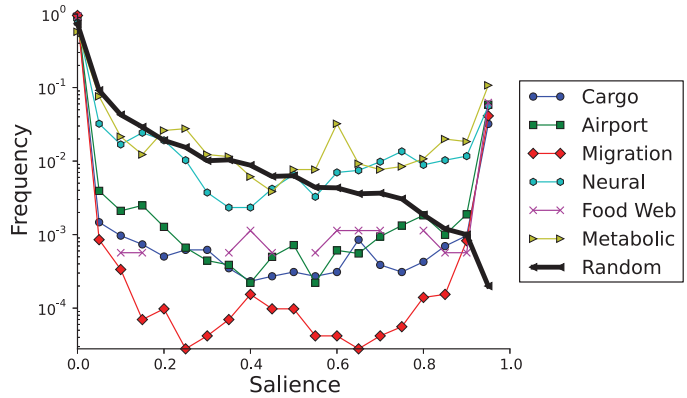

FIG. 1. The salience distribution of the networks used in the analysis. For all the networks which use real data the distribution displays a bimodal characteristic. Notably, the curve of the Random network does not have the same shape. Values not shown are at zero.

Lastly, we analyse an Erdös–Rényi network with link weights drawn from a power-law distribution (Random). Basic summary statistics for the networks, such as the number of nodes N and links L, is provided in Table 1.

1.2 *Skeleton methods*

While there are many ways to extract the most central links, the two methods explored here are the *salience skeleton* of Grady *et al.* [21] and the *disparity backbone* of Serrano *et al.* [22]. The disparity filter backbone was chosen since it is a well-established method and has been employed in many studies [23,24], whereas the salience skeleton is a more recent method with significant prospects. Further, these methods represent two fundamental classes of methods. The disparity filter is a representative statistical method, whereas the salience is a representative topological method. While these two methods do not cover all of the current possibilities they are two unique and significant methods of extracting skeletons. Both of these methods use the weights on the network links and therefore require that the data be presented as a weighted network. Note that while the terms 'backbone' and 'skeleton' are generally synonymous, for clarity we will refer to the *salience skeleton* and *disparity filter backbone* for these methods.

The salience skeleton is an analysis based on the shortest path trees (SPTs) of a network and is similar to the method used by Wu *et al.* [25] to find superhighways. First we compute the SPT, T_i, rooted at each node, i, of the network using Dijkstra's algorithm. The tree contains the collection of links that are present in at least one shortest path from node i to another node in the network. This tree can be represented as a matrix $\mathbf{T_i}$ with elements $T_{nm,i}$ such that $T_{nm,i} = 1$ if link nm is part of the tree of node i and $T_{nm,i} = 0$ otherwise. The salience is defined as the expected SPT, i.e. $\mathbf{S} = \langle \mathbf{T} \rangle$, explicitly

$$S_{nm} = \frac{1}{N} \sum_{i}^{N} T_{nm,i}. \tag{1.1}$$

In real networks salience is distributed bimodally (Fig. 1), meaning that links occur in nearly all SPTs ($S \approx 1$) or in almost none ($S \approx 0$). This makes it a natural way of extracting a network skeleton without having to choose an arbitrary cutoff for S. Note that Equation (1.1) is very similar to edge betweenness but subtly distinct in that it counts each *tree* whereas betweenness counts each *path* [21].

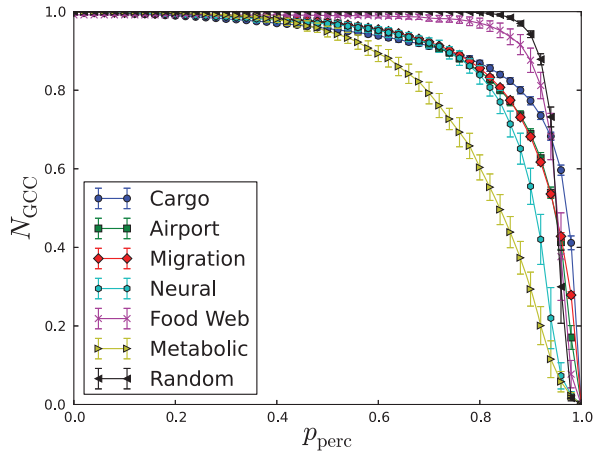

FIG. 2. The GCC under link percolation. We observe that the fraction of nodes in the GCC, N_{GCC}, of the network is robust under link percolation meaning most links must be removed before the network fragments. This holds for all networks studied here.

The disparity backbone method focuses on statistically significant deviations in link weight. One begins by defining a null model that determines the expected distribution of link weights around a node with k links if those weights were distributed randomly. The method then compares the actual link weights around the node to the null model. A significance level $\alpha \in (0, 1)$ is chosen and all links that are statistically significant at α belong to the disparity backbone [22]. More explicitly, we examine for each node, i and j, of an edge ij, if

$$\alpha_{ij} = 1 - (k-1)\int_0^{p_{ij}} (1-x)^{k-2}\,\mathrm{d}x = (1-p_{ij})^{k-1} < \alpha, \tag{1.2}$$

where k is the degree of the node examined, $p_{ij} = w_{ij}/\sum_i w_{ij}$ is the weight of the edge normalized by the strength of the node and α is a chosen significance level. In this case, α_{ij} is the p-value of the edge which is then compared with the significance level desired. If $\alpha_{ij} < \alpha$ for either node i or j, then the edge ij is kept in the skeleton, otherwise the edge is left out [22].

1.3 *Robustness methods*

In perturbing the networks, we explore (i) node percolation, (ii) link percolation and (iii) link switching. We define the percolation either of links or nodes by the number p_{perc} which is the fraction of links or nodes removed from the network. The classic result from percolation involves a phase transition in the size of the giant connected component (GCC) for random networks. For most real networks, there is no phase transition (while $p_{\mathrm{perc}} < 1$) and the size of the GCC is robust. We repeat this experiment and examine how the GCC changes under link percolation for our datasets. In Fig. 2, we confirm the previous results, which have shown that real networks are robust to link percolation.

There are a variety of methods of performing link rewiring and the process is somewhat subtle. We use the method introduced by Karrer *et al.* [26], which involves rewiring in such a way that the expectation value of the degree of each node is preserved. This is done by defining the probability of an edge, e_{ij}, existing between nodes i and j according to their degrees:

$$e_{ij} = \frac{k_i k_j}{2L}, \tag{1.3}$$

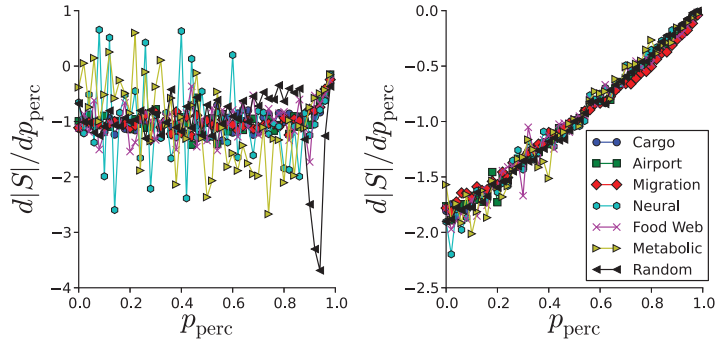

FIG. 3. How site (or node) percolation changes the size of the (left) salience skeleton and the (right) disparity backbone. The linear decrease in the size of the skeleton as p_{perc} increases shows that the size of the skeleton is proportional to N, the number of nodes in the network. (The noise in the Neural and Metabolic networks is likely due to the smaller size of those networks.) Meanwhile, the disparity backbone decreases in size more quickly than the salience skeleton for $p_{\text{perc}} < \frac{1}{2}$. The disparity backbone is more sensitive to site percolation than the salience skeleton, especially for small amounts of percolation.

where k_i is the degree of node i. To rewire, we go through each edge in the network and with some probability p_s we remove that edge and insert a new edge between nodes i and j, with i and j chosen with probability e_{ij}/L. Otherwise, with probability $1 - p_s$, we leave that original edge in place. Karrer *et al.* show that this rewiring scheme preserves the expected degree of each node in the network while allowing us to tune the quantity of randomness with the parameter p_s.

2. Results

We now study how our skeleton methods perform in the face of noisy and missing data by applying them to perturbed versions of our networks and comparing their results to those obtained for the original networks. For each value of p_{perc} with a given skeleton and perturbation method, we average the results over 100 trials and plot the mean and standard deviation. We note that rather than plotting $|S|$ vs. p_{perc} we plot $\mathrm{d}|S|/\mathrm{d}p_{\text{perc}}$ vs. p_{perc} in order to more closely reveal changes in the size of the skeleton. Numerically, we calculate this quantity as the discrete derivative

$$\frac{\mathrm{d}|S|}{\mathrm{d}p_{\text{perc}}} = \frac{|S(p_{\text{perc}_2})| - |S(p_{\text{perc}_2})|}{\Delta p_{perc}}, \tag{2.1}$$

where $|S(p_{\text{perc}_2})| - |S(p_{\text{perc}_2})|$ represents the change in the size of the skeleton between two values of p_{perc}.

In the case of node percolation, we observe that the size or fraction of links in the skeleton, $|S|$, is roughly proportional to N, the number of nodes in the network. This can be seen by the fact that $\mathrm{d}|S|/\mathrm{d}p_{\text{perc}} \approx -1$. For the salience skeleton, this is true for all values of p_{perc} while for the disparity backbone the linear regime terminates earlier. This is shown in Fig. 3. This suggests that for the salience skeleton it is mainly the path to the removed node that is affected by the percolation while paths to other nodes may change slightly but contain about the same number of links as the original path. For the disparity backbone, the decrease is faster than for the salience skeleton which shows that the size of the disparity backbone is more sensitive to the number of nodes in the network.

In examining changes to the links in the network, we look at several other quantities. First the skeleton GCC, S_{GCC} is intuitively defined as the fraction of the network that is connected when the network is

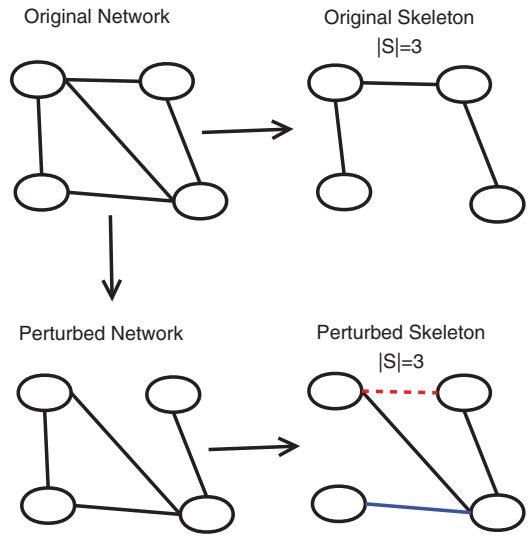

FIG. 4. The skeleton of the original network is computed with $|S|$ being defined as the number of links in the skeleton. After this, the original network is perturbed either through percolation or link switching and the new skeleton is calculated. In the bottom right network, the upper dotted link represents a link present in the original skeleton that was deleted in the new skeleton, so $L_D = 1$ for this example. In contrast, the bottom link represents a link present in the new skeleton but not the old skeleton, i.e. a link added so $L_A = 1$.

reduced to its skeleton. Secondly, we examine how many links are added to the skeleton, L_A, after perturbation, and how many links are deleted from the skeleton, L_D, after perturbation. An explanation of the quantities L_A and L_D is shown graphically in Fig. 4. It is also important to note that the comparisons for L_A and L_D are always made to the original skeleton.

For link percolation, we observe in Fig. 5 that for the salience skeleton both the size of the skeleton and the size of the skeleton GCC (S_{GCC}) are robust to change. However, the plots of L_A and L_D make clear that the salience skeleton itself is undergoing significant changes. Essentially this suggests that under link percolation the salience skeleton is able to find replacement pathways and those paths are not considerably longer than the original paths. Links are being added and deleted, yet the skeleton is simply rerouted and maintains its connectivity and size.

The one exception to this is the simulated Random network which has a very fragmented skeleton. This behaviour corresponds to the fact that in the Random network there is a weaker preference for shortest paths, i.e. the salience is not bimodal as shown in Fig. 1. However, after we remove a large fraction of the links each node only has a couple of links and the shortest paths all go through the same links.

To analyse this hypothesis and confirm that this is not an artefact of the specific salience cutoff value chosen (0.5), we examine the S_{GCC} of the Random network with different salience cutoff values. In Fig. 6, we observe that the S_{GCC} vs. p_{perc} curve has the same shape until the salience cutoff is very low. At that point the S_{GCC} of the Random network is also robust to percolation and increasing the amount of percolation never leads to a larger S_{GCC}. The different behaviour of the Random network shows that real networks have intrinsic properties which lead the S_{GCC} to be robust under link percolation.

Meanwhile, in Fig. 7 we consider how link percolation affects the disparity backbone. The backbone size decreases, yet its GCC remains robust. Comparing L_A with L_D shows that many links are deleted

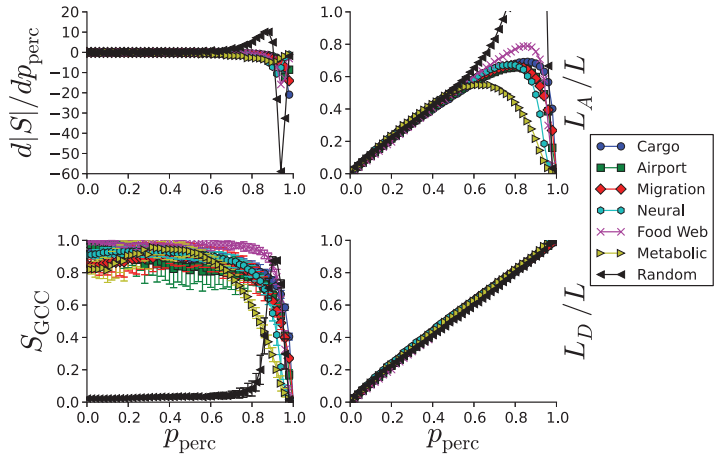

FIG. 5. Changes to the salience skeleton under link percolation. (top left) The size of the skeleton is robust to link percolation since $\mathrm{d}|S|/\mathrm{d}p_{\mathrm{perc}} \approx 0$ until $p_{\mathrm{perc}} \to 1$. (bottom left) The GCC of the skeleton itself is also robust to link percolation (except in the case of the random network). This is similar to the giant component of the network as a whole which was previously shown to be robust to link percolation. (top right) Despite the robustness of the size of the skeleton, there are many new links that are added to the skeleton as we increase p_{perc}. (bottom right) Further, we observe that an equivalent number of links are removed from the skeleton which leads to the lack of change in its size. This demonstrates that the skeleton performs a balancing act where removed links are compensated with new links. New shortest paths are found and these new paths contain approximately the same number of links as the old ones.

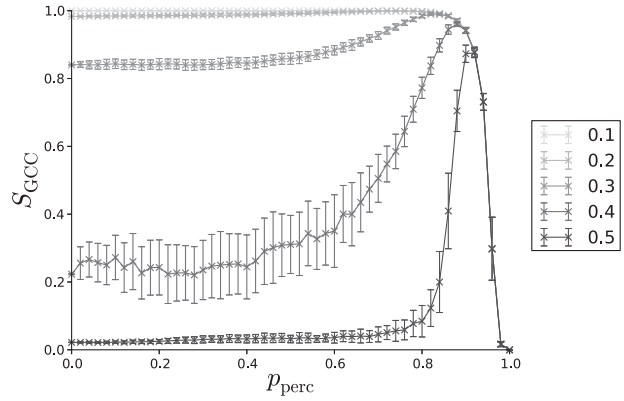

FIG. 6. The skeleton GCC, S_{GCC}, of the Random network with different salience cutoffs. For salience cutoff values > 0.3, the S_{GCC} increases at $p_{\mathrm{perc}} \approx 0.8$ and then begins decreasing at $p_{\mathrm{perc}} \approx 0.95$. The unique shape of the salience distribution of the Random network leads to different cutoffs being required for robustness.

and very few are added to compensate for those removed. We also observe that the backbone of the Random network is less robust than the backbones of the real networks, as it was for the salience skeleton.

Similarly, upon switching links using the method of Karrer *et al.* [26], we observe that S and S_{GCC} are robust for both the salience skeleton (Fig. 8) and the disparity backbone (Fig. 9). The significant decrease and large variation in the Airport network's salience skeleton giant component are likely due

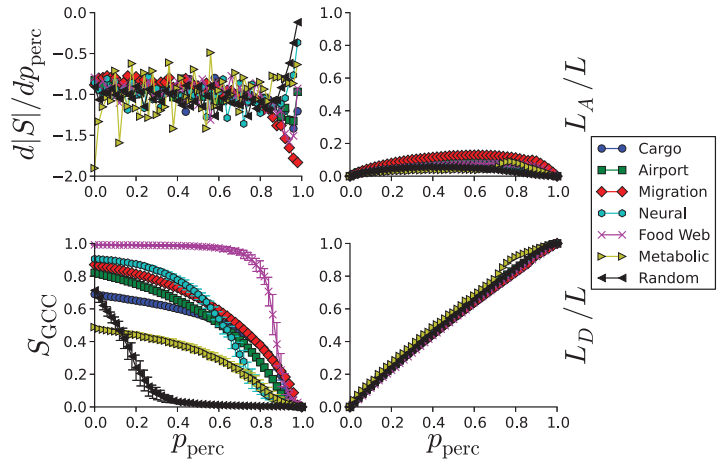

FIG. 7. Changes to the disparity backbone under link percolation. (top left) The size of the backbone is not robust to link percolation which is in contrast to the salience skeleton. (bottom left) In agreement with the salience skeleton, the GCC of the disparity backbone is also robust to link percolation, yet not quite to the same extent. (top right) Relatively few links are added to the disparity backbone as links are deleted. Again, this is in contrast to the salience skeleton where enough links were added to compensate for the links deleted from the skeleton. (bottom right) The rate at which links are deleted from the backbone is similar to that for the salience skeleton. The main difference, however, is that this removal of links is not compensated for by the addition of new links.

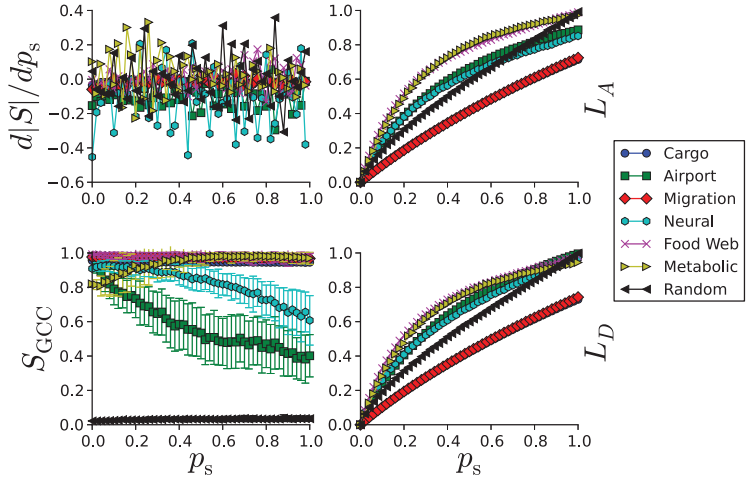

FIG. 8. Changes to the salience skeleton under link switching. (top left) The size of the skeleton is again robust. (bottom left) The skeleton giant component of most of the networks is robust to link switching, yet the Airport network's skeleton becomes dramatically fragmented. This is likely due to a specific, unstable hierarchical (or hub-spoke) structure present in the Airport network that dictates the paths for the salience skeleton. Such a hub-spoke structure may also account for the slight decrease in the skeleton size for the neural network. (top and bottom right) Many links are added and removed from the skeleton, once again in a way that maintains its size. Further, this reveals that while the size of the skeleton can be determined by the number of nodes and the degree distribution, knowing which particular links will be present in the skeleton requires having the complete dataset.

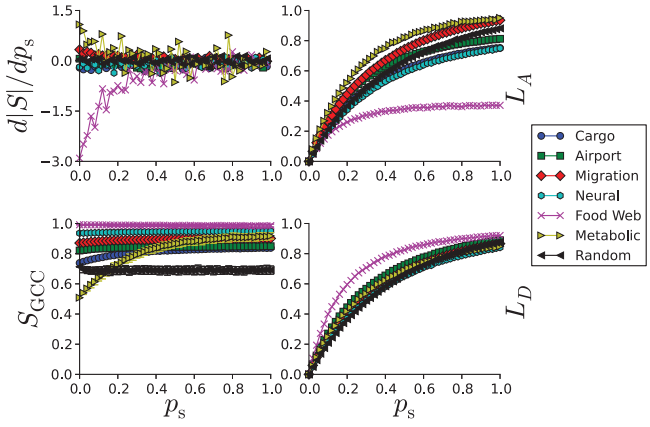

FIG. 9. Changes to the disparity backbone under link switching. (top left) As was true for the salience skeleton under link switching and link percolation, we find the size of the disparity backbone to be robust under link switching. (bottom left) The GCC of the disparity backbone is similarly robust. (top and bottom right) Again there are a significant number of links added and deleted yet they once again balance to maintain the size of the skeleton.

to a specific, unstable hierarchical structure present in that network which, when altered, leads to fragmentation. Further work is needed to determine the exact nature of this structure. The Neural network exhibits similar behaviour likely due to this. The low S_{GCC} of the Random network occurs for the same reason as seen under link percolation. Once again, we observe that similar to link percolation, despite the robustness of the skeleton size and GCC, there are significant changes in the links that actually make up the skeleton. Specifically, we see large changes in L_A and L_D just as we did with link percolation.

3. Conclusion

These results show that global summary statistics of skeletons, such as the size of the skeleton and the size of the skeleton GCC, are robust to changes in the network structure. In contrast, the specific details of the skeleton, such as the exact links it contains, will vary, potentially greatly, as the network is perturbed. This suggests that while skeleton extraction methods are useful for understanding the global properties of a network, caution should be applied when attempting to understand local properties based on extraction methods.

We further showed that different methods of computing the skeleton respond quite differently under perturbation in many cases. This suggests that caution must be applied before applying these results to yet untested methods. Nonetheless, these results do suggest that basic global statistics can be extracted regardless of the method. Lastly, the response of skeletons of real networks is significantly different than the response of a random network. The methods used to compute network skeletons and backbones exploit properties of real networks and these properties are not present in the simulated network. This leads the skeleton of the Random network to respond quite differently under perturbation.

An obvious application of this work is to damage or change in transportation networks, where skeletons will be responsible for carrying the majority of the system's traffic. This change often occurs in the real-world scenario of transport reroutings and cancellations. The results here show that as these changes occur the specific composition of the backbone or skeleton changes significantly. Nonetheless global properties can still often be extracted from the skeleton.

A second application is in protein–protein networks. These networks often contain noisy data and are considered incomplete in the interactions they show [27,28]. Significant work to map these networks entirely and obtain a full set of all the connections present is ongoing [29]. Despite the lack of the full dataset, much analysis has already been done on the data that is available [30,31]. Our results suggests that caution should be applied when looking at structural skeletons or backbones for many biological datasets that contain noisy data because the errors will have a profound impact on the resulting skeleton and backbone structures.

Lastly, these results have implications for temporal networks. In this case, it is not that our knowledge is lacking about the network, but that the links change as time progresses [32]. Social networks often display this sort of time dependence [33] and many neural networks also change through time [34,35]. For these networks caution must be taken before applying methods of extracting skeletons or backbones since their changing states will lead to different results.

Funding

This work was supported by the Volkswagen Foundation.

References

1. Albert, R. & Barabási, A. L. (2002) Statistical mechanics of complex networks. *Rev. Mod. Phys.*, **74**, 47–97.
2. Milo, R., Shen-Orr, S., Itzkovitz, S., Kashtan, N., Chklovskii, D. & Alon, A. (2002) Network motifs: simple building blocks of complex networks. *Science*, **298**, 824–827.
3. Newman, M. E. (2003) The structure and function of complex networks. *SIAM Rev.*, **45**, 268–276.
4. Strogatz, S. (2001) Exploring complex networks. *Nature*, **410**, 268–276.
5. Ahn, Y.-Y., Bagrow, J. P. & Lehmann, S. (2010) Link communities reveal multiscale complexity in networks. *Nature*, **466**, 761–764.
6. Motter, A. E. & Albert, R. (2012) Networks in motion. *Phys. Today*, **65**, 43.
7. Bullmore, E. & Sporns, O. (2009) Complex brain networks: graph theoretical analysis of structural and functional systems. *Nat. Rev. Neurosci.*, **10**, 186–198.
8. Guimerá, R., Mossa, S., Turtschi, A. & Amaral, L. (2004) The worldwide air transportation network: anomalous centrality, community structure, and cities' global roles. *Proc. Natl Acad. Sci.*, **102**, 7794–7799.
9. Kaluza, P., Kolzsch, A., Gastner, M. & Blasiuis, B. (2010) The complex network of global cargo ship movements. *J. R. Soc.*, **7**, 1093–1103.
10. Gfeller, D. & De Los Rios, P. (2007) Spectral coarse graining of complex networks. *Phys. Rev. Lett.*, **99**, 038701.
11. Albert, R., Jeong, H. & Barabási, L. (2000) Error and attack tolerance of complex networks. *Nature*, **406**, 378–382.
12. Cohen, R., Erez, K., ben Avraham, D. & Havlin, S. (2000) Resilience of the Internet to random breakdowns. *Phys. Rev. Lett.*, **85**, 4626–4628.
13. Callaway, D. S., Newman, M. E. J., Strogatz, S. H. & Watts, D. J. (2000) Network robustness and fragility: percolation on random graphs. *Phys. Rev. Lett.*, **85**, 5468–5471.
14. Newman, M. E. J. & Watts, D. J. (1999) Scaling and percolation in the small-world network model. *Phys. Rev. E*, **60**, 7332–7342.
15. Barrat, A., Barthélemy, M., Pastor-Satorras, R. & Vespignani, A. (2004) The architecture of complex weighted networks. *Proc. Natl Acad. Sci.*, **101**, 3747–3752.
16. Colizza, V., Barrat, A., Barthélemy, M. & Vespignani, A. (2006) The role of the airline transportation network in the prediction and predictability of global epidemics. *Proc. Natl Acad. Sci.*, **103**, 2015–2020.

17. White, J. G., Southgate, E., Thomson, J. N. & Brenner, S. (1986) The structure of the nervous system of the nematode caenorhabditis elegans. *Philos. Trans. R. Soc. London. B, Biol. Sci.*, **314**, 1–340.

18. Watts, D. J. & Strogatz, S. H. (1998) Collective dynamics of 'small-world' networks. *Nature*, **393**, 440–442.

19. Ulanowicz, R. E., Bondavalli, C. & Egnotovich, M. S. Network analysis of trophic dynamics in south Florida ecosystem, fy 97: The Florida bay ecosystem (1998). http://www.cbl.umces.edu/~atlss/FBay701.html.

20. Almaas, E., Kovacs, B., Vicsek, T., Oltvai, Z. & Barabási, A.-L. (2004) Global organization of metabolic fluxes in the bacterium Escherichia coli. *Nature*, **427**, 839–843.

21. Grady, D., Thiemann, C. & Brockmann, D. (2012) Robust classification of salient links in complex networks. *Nat Commun*, **3**, doi:10.1038/ncomms1847.

22. Serrano, M., Boguñá, M. & Vespignani, A. (2009) Extracting the multiscale backbone of complex weighted networks. *Proc. Natl Acad. Sci.*, **106**, 6483–6488.

23. Serrano, M. Á., Boguñá, M. & Sagués, F. (2012) Uncovering the hidden geometry behind metabolic networks. *Mol. BioSyst.*, **8**, 843–850.

24. Radicchi, F., Ramasco, J. J. & Fortunato, S. (2011) Information filtering in complex weighted networks. *Phys. Rev. E*, **83**, 046101.

25. Wu, Z., Braunstein, L., Havlin, S. & Stanley, H. (2006) Transport in weighted networks: partition into superhighways and roads. *Phys. Rev. Lett.*, **96**, 148702.

26. Karrer, B., Levina, E. & Newman, M. E. J. (2008) Robustness of community structure in networks. *Phys. Rev. E*, **77**, 046119.

27. Jansen, R., Yu, H., Greenbaum, D., Kluger, Y., Krogan, N., Chung, S., Emili, A., Snyder, M., Greenblatt, J. & Gerstein, M. (2003) A Bayesian networks approach for predicting protein protein interactions from genomic data. *Science*, **302**, 449–453.

28. von Mering, C., Krause, R., Snel, B., Cornell, M., Oliver, S., Fields, S. & Bork, P. (2002) Comparative assessment of large scale data sets of protein protein interactions. *Nature*, **417**, 399–403.

29. Tong, A. H. Y., Lesage, G., Bader, G. D., Ding, H., Xu, H., Xin, X., Young, J., Berriz, G. F., Brost, R. L., Chang, M. *et al.* (2004) Global mapping of the yeast genetic interaction network. *Science*, **303**, 808–813.

30. Bu, D., Zhao, Y., Cai, L., Xue, H., Zhu, X., Lu, H., Zhang, J., Sun, S., Ling, L., Zhang, N. *et al.* (2003) Topological structure analysis of the protein protein interaction network in budding yeast. *Nucleic Acids Res.*, **31**, 2443–2450.

31. Han, J. J., Bertin, N., Hao, T., Goldberg, D. S., Berriz, G. F., Zhang, L. V., Dupuy, D., Walhout, A., Cusick, M. E., Roth, F. P. *et al.* (2004) Evidence for dynamically organized modularity in the yeast protein–protein interaction network. *Nature*, **430**, 88–93.

32. Holme, P. & Saramäki, J. (2012) Temporal networks. *Phys. Rep.*, **519**, 97–125.

33. Pacheco, J. M., Traulsen, A. & Nowak, M. A. (2006) Coevolution of strategy and structure in complex networks with dynamical linking. *Phys. Rev. Lett.*, **97**, 258103.

34. Fabri, S. & Kadirkamanathan, V. (1996) Dynamic structure neural networks for stable adaptive control of nonlinear systems. *Neural Networks, IEEE Transactions on Systems, Man, and Cybernetics*, **7**, 1151–1167.

35. Wu, S. & Er, M. J. (2000) Dynamic fuzzy neural networks-a novel approach to function approximation. *IEEE Transactions on Systems, Man, and Cybernetics*, **30**, 358–364.